Analytical prediction of the phase change front movement to characterize tube in tube phase change material heat exchangers

Maité Goderis[a,b], Julie Van Zele[a], Kenny Couvreur[a,b], Wim Beyne[a,b] and Michel De Paepe[a,b]

[a] *Department of Electromechanical, Systems and Metal Engineering – UGent, Ghent, Belgium, Maite.Goderis@UGent.be*
[b] *FlandersMake@UGent – Core lab EEDT-MP, Leuven, Belgium, www.flandersmake.be*

Abstract

Tube in tube phase change material (PCM) heat exchangers have great potential as latent thermal energy storage (LTES) systems. However, sizing and designing these systems is still a challenge. Standard heat exchanger models cannot be applied due to the non-linear and transient heat transfer behavior of the PCM. Several alternative methods are suggested but these models are unable to predict the complete outlet state as a function of time. To fill this gap, an analytical model is derived to estimate the phase change front position as a function of time. It is proposed that the time the front needs to reach a certain vertical position is a linear function of the position. To validate the proposed analytical model, experiments are performed on a vertical tube in tube heat exchanger with varying inlet conditions. In the inner tube, water flows as heat transfer fluid (HTF). A paraffin is used as PCM in the outer tube. The phase change front position is evaluated at the outside of the tube. The movement of the phase change front is represented by plotting the vertical position of the front as a function of time. The position of the front is determined based on visual measurements using a camera placed next to the tube. By predicting the front position as a function of time, the performance of the heat exchanger can be determined. Different designs can be compared more easily, without needing to experimentally test or simulate, leading to a shorter and less expensive design phase for LTES systems, enhancing their large-scale roll-out.

Keywords:

Latent thermal energy storage; Phase change material; Tube in tube; Phase change front.

1. Introduction

Latent thermal energy storage (LTES) systems are regarded as an effective means of storing thermal energy, utilizing phase change materials (PCMs) that absorb or release energy during the phase change. The European Union (EU) has set ambitious goals concerning energy efficiency and reducing carbon emissions [1, 2]. To reach these goals, the EU has made energy storage systems one of its research goals [2]. Especially thermal energy storage systems are of paramount importance, as 50% of our energy use is thermal [3]. LTES systems offer an effective way to store thermal energy, which is beneficial in reducing energy consumption during peak demand periods and can help in the reduction of reliance on fossil fuels.

Different types of LTES systems exist. A distinction can be made between systems that use or do not use heat transfer fluids (HTFs) to exchange heat or cold [4]. In this paper, the focus is on LTES systems that use HTFs: LTES heat exchangers. Different geometries are possible but the shell and tube configuration is the most commonly used [5].

However, designing an effective LTES heat exchanger can be challenging. The key design problem requires determining the heat transfer rate from HTF to PCM (or from PCM to HTF) as a function of time and the outlet HTF temperature as a function of time, based on the system's geometrical and operational conditions [6]. When designing conventional heat exchangers, the effectiveness-number of transfer units (NTU) and logarithmic mean temperature difference (LMTD) methods can be used. The methods are developed for heat exchangers which reach a steady state, implying that the local state of the heat transfer fluid is no longer a function of time. However, LTES systems are transient in nature [4], consequently, these methods are not applicable to such systems.

Previous attempts have been made to develop analytical methods that are suitable for LTES heat exchanger design. Some of the methods that have been proposed are the average effectiveness method, which was

https://doi.org/10.52202/069564-0191

introduced by Tay et al. [6, 7], and the phase change time method proposed by Raud et al. [8]. However, these methods only allow an estimation of a specific aspect of the outlet state of an LTES heat exchanger. Another approach is the charging time energy fraction method (CTEFM) method developed by Beyne et al. [9], which allows the outlet HTF temperature to be estimated as a function of time. However, this method cannot be used as a design method, as fitting to experimental data is required. Alternatives such as purely experimental methods and Computational Fluid Dynamics (CFD) based design are often too expensive and time-consuming.

Despite the above-mentioned efforts, there is still a gap in LTES heat exchanger design methodology. Therefore, there is a need for further research to develop more accurate and cost-effective analytical methods that can be used to design LTES heat exchanger systems with high efficiency and performance, for specific applications.

Recently, Beyne et al. [10] developed an analytical solution to predict the performance of LTES heat exchangers based on the heat transfer model of a cross section. A model is used for the local heat transfer under constant boundary conditions, based on the solution to the Stefan problem. In the Stefan problem, sensible heat is neglected compared to the latent heat of the PCM and the phase change is assumed to occur isothermally. The phase change problem is considered purely conductive and the PCM properties are assumed independent of the temperature. Computation of the phase change front location as a function of time allows determining the phase change fraction as a function of time. This relates to the PCM internal energy per unit of heat transfer surface. Next, this solution is integrated to determine the overall phase change fraction of the complete LTES heat exchanger. In [10] this analytical solution is verified for a planar geometry by comparing it to a numerical simulation. The results had small average deviations for the phase change fraction and effectiveness. The total phase change time was very well predicted.

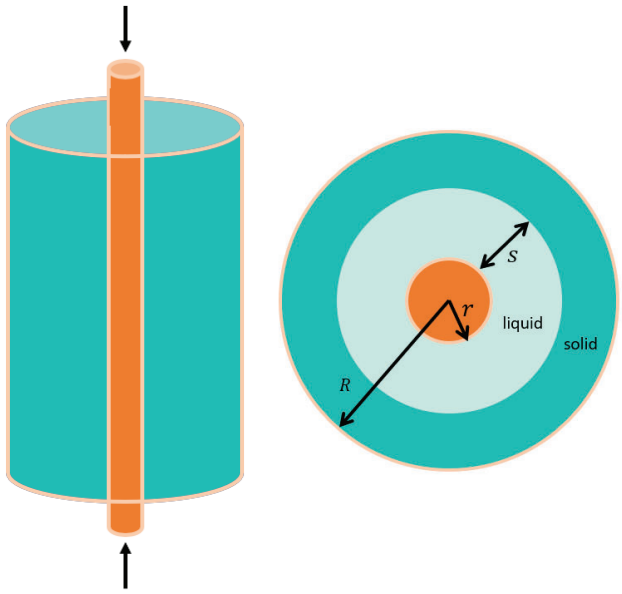

Figure 1. Schematic of tube in tube system during phase change.

In this paper, the proposed analytical method will be evaluated based on experimental data of a tube in tube LTES heat exchanger. The geometry is schematically shown in Figure 1. Similar to the planar geometry, analytical equations can be derived to predict the phase change front behavior as a function of time, now for a cylindrical geometry. The overall phase change fraction of a tube in tube heat exchanger can be determined based on the position of the phase change front in a cylindrical cross-section with constant boundaries, which relates to the PCM internal energy per unit of heat transfer surface. When this solution is integrated over the heat exchanger, the overall phase change fraction of the complete LTES system can be determined.

Beyne et al. [10] states that the phase change front moves linearly in time over the length of the tube. The time for the front to reach a certain vertical position $x = x_1$ is then given by Equation 1. The x-axis indicates the position of the phase change front at the outer diameter of the tube, as indicated in Figure 2.

$$t(x_1) = t_0 + \sigma . x_1 \qquad 1$$

t_0 is the time that is needed for the phase change front to reach the outer diameter of the PCM tube for the first time, thus at height $x = 0$. The slope σ can be estimated as in Equation 2. U_a is the latent heat of phase change of the PCM per length unit. $\dot{m}$ and c_p are respectively the mass flow rate and specific heat capacity of

https://doi.org/10.52202/069564-0191

the HTF, and ΔT_0 is the temperature difference between the HTF temperature at the inlet and the PCM phase change temperature.

$$\sigma = \frac{U_a}{\dot{m} c_p \Delta T_0} \quad (2)$$

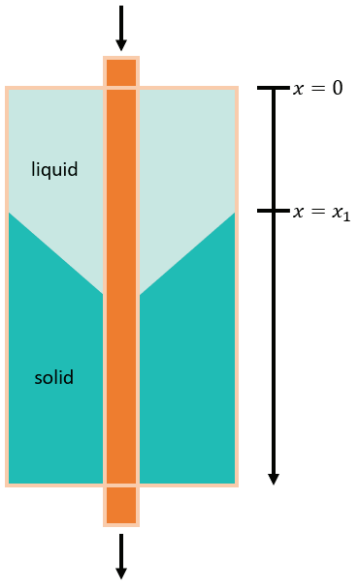

Figure 2. Section of tube in tube heat exchanger with phase change front schematically shown.

Mehling and Cabeza [11] provide a correlation for the radial movement of the phase change front in a one-dimensional cylindrical geometry. This correlation is based on the solution to the Stefan problem. Equation 3 denotes the time t that is needed for the phase change front to move a distance s away from the HTF tube with radius r. Equation 3 can be split up into two factors. The first factor relates the front position s to the phase change fraction, defined based on the latent heat of phase change the PCM h_{lat}, the density of the PCM ρ_{PCM}, the thermal conductivity k of the PCM and the temperature difference ΔT_0 between HTF temperature at the inlet and the phase change temperature of the PCM. The second factor f is a function of the ratio of the thermal conductivity k of the PCM to the convective heat transfer coefficient h of the HTF and the radial front position s. This factor describes the deviation of the solution compared to the solution of the Stefan problem, due to the boundary effects of the HTF. For the considered tube in tube heat exchanger, the second factor can be calculated as in Equation 4. It is assumed that the thickness of the HTF tube wall is much smaller than the outer HTF tube radius r and that the conductivity of the HTF wall is much larger than the conductivity of the PCM. These assumptions apply to the considered experimental setup (see Section 2). Equation 3 can be used to calculate t_0 in Equation 1, by defining $s = R - r$.

$$t(s) = \frac{h_{lat} \cdot \rho_{PCM} \cdot s^2}{2 \cdot k \cdot \Delta T_0} \cdot f\left(s, \frac{k}{h}\right) \quad (3)$$

$$f\left(s, \frac{k}{h}\right) = \left(1 + \frac{r}{s}\right)^2 \ln\left(1 + \frac{s}{r}\right) - \left(1 + \frac{2r}{s}\right)\left(\frac{1}{2} - \frac{k}{h\,r}\right) \quad (4)$$

A series of experiments on a tube in tube heat exchanger are conducted while the position of the phase change front is tracked over time. The observed results regarding the phase change front position are compared to the expected front position, based on the correlations from Beyne et al. [10] and Mehling and Cabeza [11], mentioned above. The accuracy of the proposed analytical model is investigated.

2. Setup description

The heat exchanger tested, is a tube in tube configuration with a length of one meter, which is oriented vertically to take advantage of the axisymmetry [12]. In this configuration, the heat transfer fluid (HTF) flows through the inner tube, while the PCM is located in the shell region. The direction of flow of the HTF can be changed using two three-way valves. During the melting process, the HTF flows from the top of the heat exchanger to the bottom. During the solidification process, it flows in the opposite direction to limit thermal stresses imposed by the PCM volume change.

The HTF flows through a copper tube with an outer diameter of 15 mm and a wall thickness of 2 mm. The copper tube is positioned concentrically within a transparent polycarbonate tube, which houses the PCM. The

shell has an outer diameter of 60 mm and a wall thickness of 3 mm. In the experiments, the paraffin RT35HC provided by Rubitherm [13] is used. This nontoxic PCM has a high thermal storage capacity and stable performance during the phase change cycles. An overview of the properties of RT35HC can be found in Table 1. A total of 1.497 kg of PCM is used during the experiments, which corresponds to a total latent heat capacity of about 380 kJ. Water is used as HTF.

Table 1: RT35HC properties [13].

Melting area	34-36	°C
Congealing area	36-34	°C
Specific heat capacity	2	kJ/kgK
Density solid (at 25°C)	0.88	kg/l
Density liquid (at 60°C)	0.77	kg/l
Heat conductivity	0.2	W/mK
Max. operating temperature	70	°C

Figure 3. Picture of the setup: insulation box.

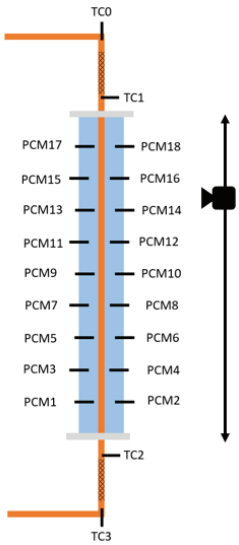

Figure 4. Schematic of the heat exchanger with camera slider, placed inside the insulation box.

A picture of the setup and a schematic of the heat exchanger be seen in respectively Figure 3 and Figure 4. Next to the tube, a camera on a linear slider is placed to allow observation of the location of the phase change front over the complete tube length. The whole of the heat exchanger and camera slider are placed in a big box filled with insulation granulates [14]. This way, thermal losses are limited in a uniform way. On the schematic, the thermocouples which are used to measure the temperature of the PCM and the HTF are indicated. The temperatures inside the PCM are measured with 18 1 mm K-type thermocouples, placed every 10 cm in the axial direction. At each height, a temperature measurement at both 0.5 and 1 cm from the outside shell wall is performed. These thermocouples are calibrated to an uncertainty of ± 0.15 °C and are acquired by a Keithley 2700 multiplexer with a sampling rate of 2.5 s. The temperatures at the HTF inlet and outlet of the heat exchanger are also measured. Mixers are inserted into the HTF tubes, ensuring the thermocouples measure the bulk HTF temperature. Before and after each mixer, a 1.5 mm K-type thermocouple was added. This way, both melting and solidification experiments can benefit from the effect of the mixers. These thermocouples are again calibrated with an uncertainty of ± 0.15 °C and are sampled with a sampling rate of 0.5 s, as the transient behavior needs to be captured. During melting, TC1 and TC3 will be used as respectively inlet and outlet of the HTF in the heat exchanger. While during solidification, this will be TC2 and TC0, as now the HTF flows from bottom to top.

https://doi.org/10.52202/069564-0191

In Figure 5 a picture taken during a melting experiment is shown. The figure includes a tape measure and a part of the transparent container, where the PCM can be seen. The transparent PCM is liquid, the white is solid.

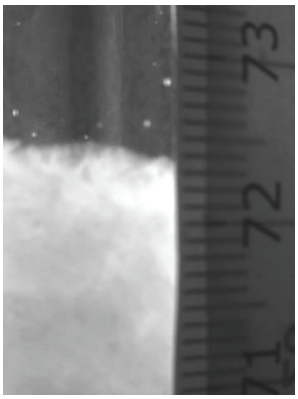

Figure 5. Picture of the phase change front during melting, taken with the camera installed next to the tube in tube heat exchanger (x = 72.4 cm).

In Table 2 an overview is given of the operational conditions of the considered melting experiments performed on the above-described setup. For each experiment, the HTF mass flow rate and two temperature differences are given. ΔT_0 quantifies the difference between the HTF inlet temperature and the phase change temperature (here assumed equal to 35 °C). ΔT_{init} is the difference between the phase change temperature and the initial temperature of the PCM. To define the initial PCM temperature, the mean of all PCM temperature measurements is used. The last column of the table gives the Reynolds number linked to the HTF.

Table 2. Overview of performed experiments.

experiment	$\dot{m}\ [kg/h]$	$\Delta T_0\ [°C]$	$\Delta T_{init}\ [°C]$	$Re\ [-]$
M1	68	26.5	8.0	4762
M2	80	25.6	14.5	5482
M3	20	22.5	17.0	1300
M4	156	19.5	10.0	9824

Only melting experiments are performed and no solidification data is taken into consideration in the context of this paper. The focus of this work is on melting experiments because during solidification tests, difficulties arise when visually observing the front. During solidification, conduction is the dominant heat transfer mode [15]. Therefore, the solidification front moves very radially from the inner shell diameter to the outside shell diameter. Because of this, it is very difficult to visually determine the moment when the front reaches the outside diameter. Similar difficulties were observed by Longeon et al. [12]. Lipnicki et al. [16] observed during their experiments that the solidification front almost has a constant radial thickness along the length of the heat exchanger, explaining the difficulties concerning determining the vertical front position at the outside of a PCM tube.

3. Results

3.1 Experimental results

As explained before, during each melting experiment, the location of the phase change front at the outer diameter of the heat exchanger is tracked over time. The position of the phase change front is normalized to the total height of the PCM ($L_{PCM} = 0.93m$), as in Equation 5. L_{PCM} is a bit smaller than 1m, as the tube is not completely filled with storage material to allow volume expansion during melting.

$$\xi = \frac{x}{L_{PCM}} \tag{5}$$

In Figure 6, the evolution of the position of the phase change front at the outer diameter of the PCM tube can be seen as a function of time, during melting experiment M1. The different melting regimes, as also observed in previous studies, can be recognised in the shape of the front-curve. In the initial phase, conduction is the

main heat transfer mode and the PCM closest to the tube will melt. As melting continues, heat transfer by convection will gain dominance and will fasten the heat transfer in the PCM. This can be seen by the steeper slope of the front-curve, meaning an increasing melting rate of the PCM when a significant part of the PCM has molten. Next, the heat transfer reaches a quasi-steady state regime with a constant heat transfer rate. The phase change front now moves linearly through the tube. Finally, when most of the PCM has molten, the shrinking solid phase starts while the heat transfer, and thus the speed with which the phase change front moves, decreases. These different melting regimes lead to the S-shape that can be recognised in the front-curve in Figure 6.

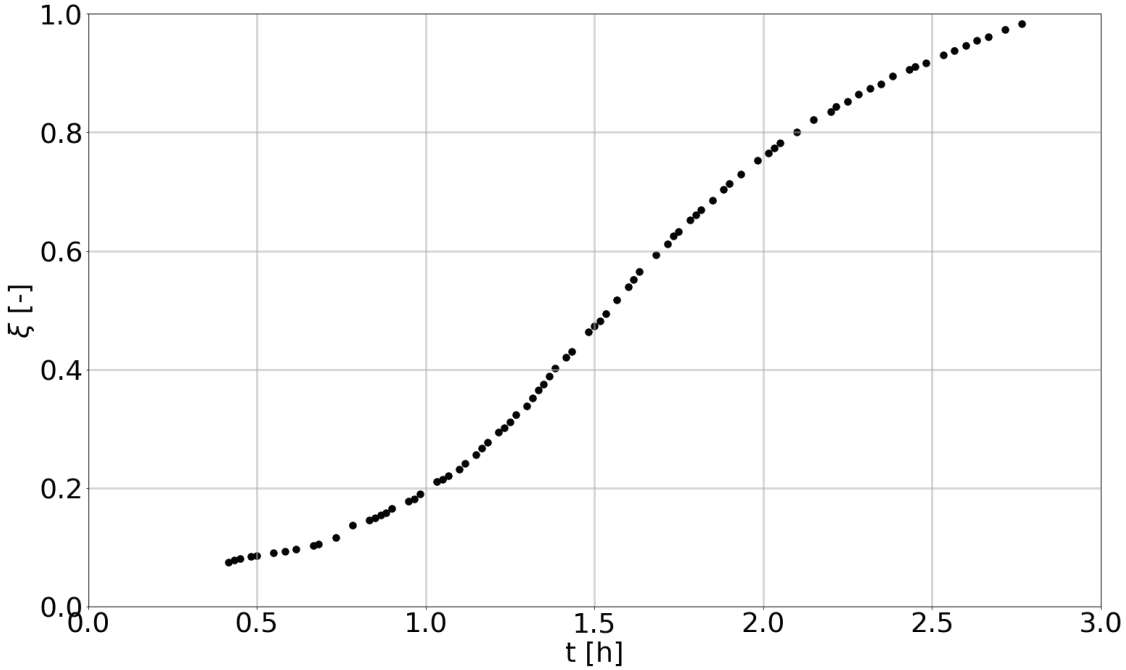

Figure 6. The evolution of the position of the phase change front at the outer radius of the PCM tube, as a function of time (melting test M1), based on the visual tracking of the phase change front position.

As mentioned above, a quasi steady-state melting regime is present during the melting process. During this phase, the melting front at the outside of the PCM tube moves linearly over time. The slope of this part of the front-curve is denoted by β for the remainder of this paper. β is only based on experimental data where ξ ranges from 0.25 to 0.65. In Figure 7 the visual, experimental data for all melting experiments is shown, and the linear approximation of the front movement during the quasi-steady melting regime is shown by the dotted black line. The linear approximation is of the shape as given in Equation 6. Some of the visual measurement points are omitted in Figure 7, to clarify the figure. The shape of the front-curve is however still obviously visible.

$$t(\xi) = \alpha + \beta \, . \, \xi \qquad 6$$

When comparing the different experimental results in Figure 7, the influence of the operational conditions can be seen. Especially increasing the temperature difference between HTF inlet temperature and the phase change temperature of the PCM, decreases the total melting time. These observations are in line with literature [17-20]. In literature is also seen that increasing the mass flow rate of the HTF, shortens the total melting time. However, when comparing experiments M1 and M2, a small increase in melting time is seen for the larger mass flow rate. Khan et al. [21] observed that for higher HTF inlet temperatures, the influence of varying the mass flow rate decreases. The shortened melting time for a larger mass flow rate can probably be explained by experimental uncertainties. The studies found in literature agreed with the observation that the heat transfer characteristics are more sensitive to a change in inlet temperature than a change in mass flow rate [22].

https://doi.org/10.52202/069564-0191

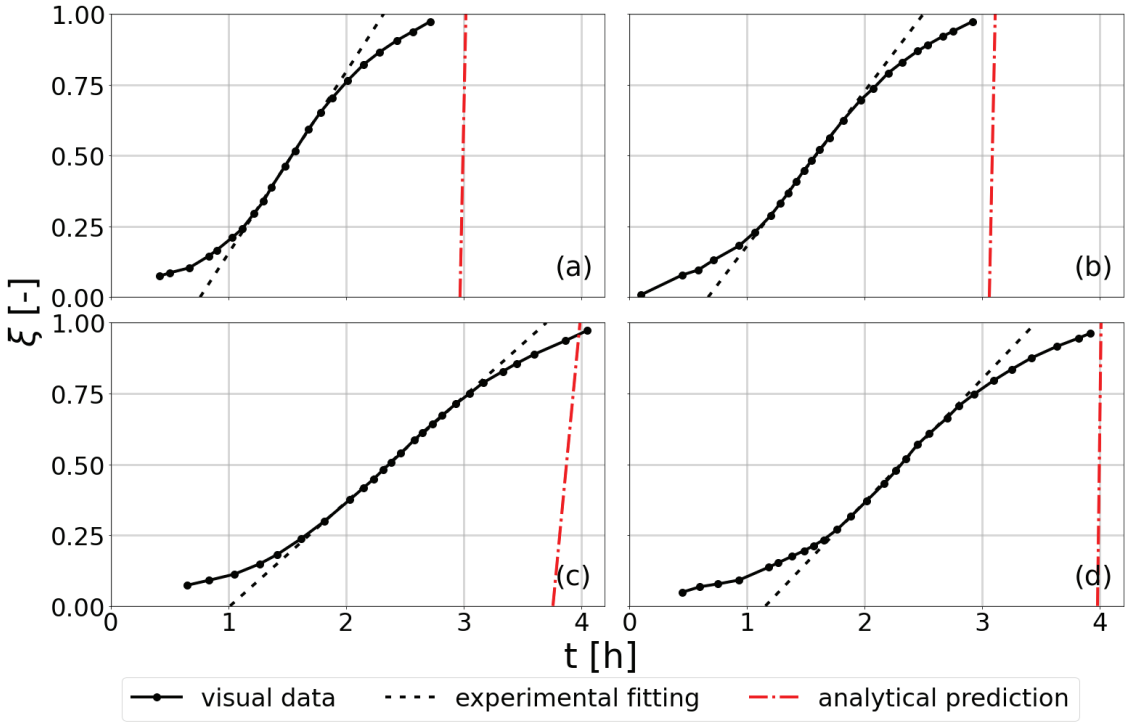

Figure 7. Experimental front data with fitted linear correlations based on β and σ for melting experiments (a) M1, (b) M2, (c) M3 and (d) M4.

3.2 Analytical correlations

As explained in Section 1, various studies propose that the phase change front moves linearly in time during melting experiments. In this Section, the analytical obtained intercept t_0 (Equation 3) is compared to the experimental α, and the analytical obtained slope σ (Equation 2) is compared to the experimental slope β, seen during the quasi-steady melting phase. Table 3 gives an overview of both intercepts and slopes for the considered operational conditions of the melting experiments of Table 2. The comparison between experimental and analytical results is visualized in Figure 7 where the black and red lines respectively represent the experimental and the analytical linear fit.

Table 3. Comparison of experimental and analytical slope.

experiment	$\boldsymbol{\alpha}$ $[\boldsymbol{h}]$	$\boldsymbol{t_0}[\boldsymbol{h}]$	$\boldsymbol{\beta}$ ***[h]***	$\boldsymbol{\sigma}$ ***[h]***
M1	1.560	2.97	0.760	0.05
M2	1.831	3.06	0.669	0.05
M3	2.689	3.76	1.015	0.23
M4	2.299	3.98	1.157	0.03

From Table 3 and Figure 4 it is clear that the proposed analytical correlations are not able to accurately predict the movement of the phase change front as a function of time of a tube in tube heat exchanger. The prediction for the total melting time is a quite an acceptable prediction. However, more experimental data is required to make any conclusions on this statement. Below some considerations are listed, explaining the deviations between experimental and analytical results.

First of all, measurement uncertainties on the measured experimental quantities must be taken into account. To calculate t_0 and σ the mean HTF inlet temperature and mean HTF mass flow rate are used. During the complete melting test, small deviations on these mean values are possible, however, these will not have a significant influence on the obtained results. The error on the visual measurements is difficult to determine but is limited to 2-3 mm. As the front position is measured every 3 minutes, this visual error will not influence the general trend of the front.

Thermal losses during the experiments could also influence the phase change front propagation. Due to the undertaken actions by installing the insulation box around the PCM heat exchanger, heat losses are limited as much as possible. Heat losses will decrease the melting rate and consequently, a faster front movement could be expected using the theoretical correlations, compared to the experimental data. However, it is improbable that the influence of the limited heat losses could be of the proportion that is seen when comparing β and σ.

Furthermore, in the derivation of the analytical correlations, only the latent heat of the PCM is considered. The sensible heat of the PCM also needs to be taken into account, as well as the heat transferred from the HTF to the container during the experiments. However, the latent heat is dominant as it is significantly larger than the other contributors to the internal energy of the system. For example for experiment M1, the latent heat of the PCM corresponds with 380 kJ, whereas the sum of the sensible PCM energy and the energy stored in the container is about 80 kJ. Including all the energy contributions would thus only have a limited influence on the value of σ.

The above-mentioned considerations concerning uncertainties in the experimental results or assumptions in determining the analytical correlations can explain a deviation between experimental and analytical results. However, the observed discrepancies cannot be explained. Therefore, a more fundamental look is taken into the analytical model, and the applicability of the model to the considered melting experiments is evaluated.

In the analytical derivation, pure conduction is assumed and the influence of natural convection is neglected, but during melting, natural convection is the dominant heat transfer mode [15]. It can thus be expected that the analytical solution will overestimate the duration of the melting process, due to the increased heat transfer during melting because of the influence of natural convection. However, the analytical prediction is a large underestimation of the experimental melting duration. A large deviation is seen between the theoretical and experimental obtained intercepts and slopes. From Table 3 and Figure 7, it is clear that the analytical slope σ is a large underestimation of the experimentally obtained β. It is predicted that the phase change front moves faster over the length of the tube, than what is visually observed.

The analytical model is based upon the assumption that the tube in tube heat exchanger can be modelled as distinct infinitesimal slices, stacked upon each other. The heat transfer behavior of the slices is assumed uncoupled. In reality, the phenomena in the different slices will be coupled, especially during melting due to vertical convection bubbles formed in the PCM. The experimental intercept α is expected to be smaller than the predicted t_0 based on purely, uncoupled conduction, due to the enhanced heat transfer because of the natural convection. This is as observed in Table 3 and Figure 7.

The analytical solution is obtained for a tube in tube heat exchanger with a temperature difference between the inlet and outlet of the heat transfer fluid. In the experiments, however, this temperature difference is rather limited. For example, for mass flow rates above $\pm 50 kg/h$ the temperature difference over the heat transfer is not measurable anymore. To validate the analytical solution, meaningful experimental data is required. To achieve this, the temperature over the heat transfer tube must be increased, by increasing the heat transfer rate between HTF and PCM. This can be done by for example adding fins to the HTF tube. However, preferably the analytical method is verified on a basic geometry. Another option to increase the heat transfer rate would be adding metal foam into the PCM to increase the effective conductivity of the storage material. Another approach could be to test a heat exchanger with an increased length. However, the height of the setup is limited due to practical limitations of the lab. In future studies, numerical simulations can be performed, eliminating the height limitations of the heat exchanger. Available experimental results can be used to fit the numerical method.

When analyzing the above-discussed results, the hypothesis arises that the analytical model can have better applicability for solidification experiments. During solidification, conduction is the dominant heat transfer mode, eliminating the deviation between experiments and model due to the influence of natural convection. Furthermore, when tracking the solidification front as a function of time, difficulties arise in determining the exact front position, because the phase change interface moves almost radially from the HTF wall to the outer PCM tube wall. The analytical model predicts such a front behavior: the predicted front moves in a couple of minutes over the complete length of the heat exchanger. In future work, solutions can be developed enabling tracking of the solidification front during experiments, or numerical simulations can be performed to validate this hypothesis.

4. Conclusions

Melting experiments are performed on a tube in tube LTES heat exchanger, with varying operational conditions. During these experiments, the location of the phase change front at the outer diameter of the PCM tube is tracked over time based on photographs. The distinct melting regimes described in literature can be seen in the obtained front movement-curve. The experimental results are compared to a predicted phase change front behavior, based on an analytical model developed by Beyne et al. [10]. It is seen that the analytical model overestimates the movement speed of the phase change front. However, a realistic estimation of the total melting time can be obtained with this model. In future work, numerical simulations are

https://doi.org/10.52202/069564-0191

recommended. Furthermore, tracking the phase change front during solidification experiments is required to validate the applicability of the analytical model for solidification.

Acknowledgment

The authors would like to express their gratitude and appreciation to the technical staff of Ghent University, especially Frederik Martens, Bart Van Daele, and Thomas Blancke for building and maintaining the setup used to obtain the discussed experimental data.

Nomenclature

c_p	specific heat capacity, J/kgK
h	convection coefficient, W/m²K
h_{lat}	latent heat of the PCM, J/kg
k	thermal conductivity, W/mK
L	length, m
m	mass, kg
$\dot{m}$	mass flow rate of HTF, kg/h
r	outer radius of HTF tube, m
R	inner radius of PCM tube, m
Re	Reynolds number, -
s	radial distance the phase change front has traveled, m
t	time, h
t_0	time the phase change front needs to reach the outer diameter of the PCM tube for the first time, h
U_a	latent heat of phase change of the PCM, per length unit, J/m
x	front position, m

Greek symbols

α	experimental intercept, h
β	experimental slope, h
ΔT_0	difference between HTF inlet temperature and PCM phase change temperature, °C
ΔT_{init}	difference between mean initial PCM temperature and PCM phase change temperature, °C
σ	analytical slope, h
ξ	dimensionless front position, -

Subscripts and superscripts

PCM	phase change material
HTF	heat transfer fluid

References

[1] "European Comission, official website." https://commission.europa.eu/index_en (accessed 17-10-2022.

[2] EUagenda. "A clean planet for all - a European long-term strategic vision for a properous, modern, competitive and climate neutral economy." https://eur-lex.europa.eu/legal-content/EN/TXT/?uri=CELEX%3A52018DC0773 (accessed 16-09-2022.

[3] IEA. "Heating - Fuels & Technologies." https://www.iea.org/fuels-and-technologies/heating (accessed 15-02-2023.

[4] A. Castell and C. Solé, "Design of latent heat storage systems using phase change materials (PCMs)," in *Advances in Thermal Energy Storage Systems*, 2015, pp. 285-305.

[5] G. S. Sodhi, V. Kumar, and P. Muthukumar, "Design assessment of a horizontal shell and tube latent heat storage system: Alternative to fin designs," *Journal of Energy Storage,* vol. 44, 2021, doi: 10.1016/j.est.2021.103282.

[6] N. H. S. Tay, M. Belusko, A. Castell, L. F. Cabeza, and F. Bruno, "An effectiveness-NTU technique for characterising a finned tubes PCM system using a CFD model," *Applied Energy,* vol. 131, pp. 377-385, 2014, doi: 10.1016/j.apenergy.2014.06.041.

[7] N. H. S. Tay, M. Belusko, and F. Bruno, "An effectiveness-NTU technique for characterising tube-in-tank phase change thermal energy storage systems," *Applied Energy,* vol. 91, no. 1, pp. 309-319, 2012, doi: 10.1016/j.apenergy.2011.09.039.

[8] R. Raud *et al.*, "Design optimization method for tube and fin latent heat thermal energy storage systems," *Energy,* vol. 134, pp. 585-594, 2017, doi: 10.1016/j.energy.2017.06.013.

[9] W. Beyne, K. Couvreur, I. T' Jollyn, R. Tassenoy, S. Lecompte, and M. De Paepe, "A charging time energy fraction method for evaluating the performance of a latent thermal energy storage heat exchanger," *Applied Thermal Engineering,* vol. 195, 2021, doi: 10.1016/j.applthermaleng.2021.117068.
[10] W. Beyne, R. Tassenoy, and M. De Paepe, "An approximate analytical solution for the movement of the phase change front in latent thermal energy storage heat exchangers," *Journal of Energy Storage,* vol. 57, 2023, doi: 10.1016/j.est.2022.106132.
[11] H. Mehling and F. L. Cabeza, *Introduction to heat and cold storage*. 2008.
[12] M. Longeon, A. Soupart, J.-F. Fourmigué, A. Bruch, and P. Marty, "Experimental and numerical study of annular PCM storage in the presence of natural convection," *Applied Energy,* vol. 112, pp. 175-184, 2013, doi: 10.1016/j.apenergy.2013.06.007.
[13] Rubitherm. "RT35HC." https://www.rubitherm.eu/media/products/datasheets/Techdata_-RT35HC_EN_09102020.PDF (accessed 13-03-2023.
[14] Deschacht. "Vermiculite." https://shop.deschacht.eu/nl-be/7921/vermiculite-g3-medium-9kg-100l (accessed 13-03-2023.
[15] M. Medrano, M. O. Yilmaz, M. Nogués, I. Martorell, J. Roca, and L. F. Cabeza, "Experimental evaluation of commercial heat exchangers for use as PCM thermal storage systems," *Applied Energy,* vol. 86, no. 10, pp. 2047-2055, 2009, doi: 10.1016/j.apenergy.2009.01.014.
[16] Z. Lipnicki and B. Weigand, "An experimental and theoretical study of solidification in a free-convection flow inside a vertical annular enclosure," *International Journal of Heat and Mass Transfer,* vol. 55, no. 4, pp. 655-664, 2012, doi: 10.1016/j.ijheatmasstransfer.2011.10.044.
[17] R. Karami and B. Kamkari, "Experimental investigation of the effect of perforated fins on thermal performance enhancement of vertical shell and tube latent heat energy storage systems," *Energy Conversion and Management,* vol. 210, 2020, doi: 10.1016/j.enconman.2020.112679.
[18] M. Esen, A. Durmus, and A. Durmus, "Geometric design of solar-aided latent heat store depending on various parameters and phase change materials," *Solar Energy,* vol. 62, no. 1, pp. 19-28, 1998, doi: 10.1016/S0038-092X(97)00104-7.
[19] M. K. Rathod and J. Banerjee, "Thermal performance enhancement of shell and tube Latent Heat Storage Unit using longitudinal fins," *Applied Thermal Engineering,* vol. 75, pp. 1084-1092, 2015, doi: 10.1016/j.applthermaleng.2014.10.074.
[20] A. Trp, K. Lenic, and B. Frankovic, "Analysis of the influence of operating conditions and geometric parameters on heat transfer in water-paraffin shell-and-tube latent thermal energy storage unit," *Applied Thermal Engineering,* vol. 26, no. 16, pp. 1830-1839, 2006, doi: 10.1016/j.applthermaleng.2006.02.004.
[21] Z. Khan and Z. A. Khan, "Experimental investigations of charging/melting cycles of paraffin in a novel shell and tube with longitudinal fins based heat storage design solution for domestic and industrial applications," *Applied Energy,* vol. 206, pp. 1158-1168, 2017, doi: 10.1016/j.apenergy.2017.10.043.
[22] L. Kalapala and J. K. Devanuri, "Influence of operational and design parameters on the performance of a PCM based heat exchanger for thermal energy storage – A review," *Journal of Energy Storage,* vol. 20, pp. 497-519, 2018, doi: 10.1016/j.est.2018.10.024.

https://doi.org/10.52202/069564-0191